

# Retinal asymmetry in multiple sclerosis

✉ Axel Petzold,<sup>1,2,3</sup> Sharon Y. L. Chua,<sup>4</sup> ✉ Anthony P. Khawaja,<sup>4</sup> ✉ Pearse A. Keane,<sup>4</sup> Peng T. Khaw,<sup>4</sup> Charles Reisman,<sup>5</sup> Baljean Dhillon,<sup>6</sup> Nicholas G. Strouthidis,<sup>4</sup> UK Biobank Eye and Vision Consortium,<sup>†</sup> Paul J. Foster<sup>4,‡</sup> and Praveen J. Patel<sup>4,‡</sup>

<sup>†</sup>Appendix 1.

<sup>‡</sup>These authors contributed equally to this work.

The diagnosis of multiple sclerosis is based on a combination of clinical and paraclinical tests. The potential contribution of retinal optical coherence tomography (OCT) has been recognized. We tested the feasibility of OCT measures of retinal asymmetry as a diagnostic test for multiple sclerosis at the community level. In this community-based study of 72 120 subjects, we examined the diagnostic potential of the inter-eye difference of inner retinal OCT data for multiple sclerosis using the UK Biobank data collected at 22 sites between 2007 and 2010. OCT reporting and quality control guidelines were followed. The inter-eye percentage difference (IEPD) and inter-eye absolute difference (IEAD) were calculated for the macular retinal nerve fibre layer (RNFL), ganglion cell inner plexiform layer (GCIPL) complex and ganglion cell complex. Area under the receiver operating characteristic curve (AUROC) comparisons were followed by univariate and multivariable comparisons accounting for a large range of diseases and co-morbidities. Cut-off levels were optimized by ROC and the Youden index. The prevalence of multiple sclerosis was 0.0023 [95% confidence interval (CI) 0.00229–0.00231]. Overall the discriminatory power of diagnosing multiple sclerosis with the IEPD AUROC curve (0.71, 95% CI 0.67–0.76) and IEAD (0.71, 95% CI 0.67–0.75) for the macular GCIPL complex were significantly higher if compared to the macular ganglion cell complex IEPD AUROC curve (0.64, 95% CI 0.59–0.69,  $P = 0.0017$ ); IEAD AUROC curve (0.63, 95% CI 0.58–0.68,  $P < 0.0001$ ) and macular RNFL IEPD AUROC curve (0.59, 95% CI 0.54–0.63,  $P < 0.0001$ ); IEAD AUROC curve (0.55, 95% CI 0.50–0.59,  $P < 0.0001$ ). Screening sensitivity levels for the macular GCIPL complex IEPD (4% cut-off) were 51.7% and for the IEAD (4  $\mu\text{m}$  cut-off) 43.5%. Specificity levels were 82.8% and 86.8%, respectively. The number of co-morbidities was important. There was a stepwise decrease of the AUROC curve from 0.72 in control subjects to 0.66 in more than nine co-morbidities or presence of neuromyelitis optica spectrum disease. In the multivariable analyses greater age, diabetes mellitus, other eye disease and a non-white ethnic background were relevant confounders. For most interactions, the effect sizes were large (partial  $\omega^2 > 0.14$ ) with narrow confidence intervals. In conclusion, the OCT macular GCIPL complex IEPD and IEAD may be considered as supportive measurements for multiple sclerosis diagnostic criteria in a young patient without relevant co-morbidity. The metric does not allow separation of multiple sclerosis from neuromyelitis optica. Retinal OCT imaging is accurate, rapid, non-invasive, widely available and may therefore help to reduce need for invasive and more costly procedures. To be viable, higher sensitivity and specificity levels are needed.

- 1 Moorfields Eye Hospital and The National Hospital for Neurology and Neurosurgery, London, UK
- 2 UCL Queen Square Institute of Neurology, London, UK
- 3 Dutch Expertise Centre for Neuro-ophthalmology and MS Centre, Departments of Neurology and Ophthalmology, Amsterdam UMC, Amsterdam, The Netherlands
- 4 NIHR Biomedical Research Centre, Moorfields Eye Hospital NHS Foundation Trust and UCL Institute of Ophthalmology, London, UK
- 5 Topcon Healthcare Solutions Research and Development, Oakland, New Jersey, USA
- 6 Centre for Clinical Brain Sciences, School of Clinical Sciences, NHS Lothian, Edinburgh, UK

Received January 27, 2020. Revised July 15, 2020. Accepted August 11, 2020. Advance access publication November 30, 2020

© The Author(s) (2020). Published by Oxford University Press on behalf of the Guarantors of Brain.

This is an Open Access article distributed under the terms of the Creative Commons Attribution Non-Commercial License (<http://creativecommons.org/licenses/by-nc/4.0/>), which permits non-commercial re-use, distribution, and reproduction in any medium, provided the original work is properly cited. For commercial re-use, please contact [journals.permissions@oup.com](mailto:journals.permissions@oup.com)

Correspondence to: Axel Petzold  
UCL Institute of Neurology, Queen Square, London, WC1N 3BG  
E-mail: a.petzold@ucl.ac.uk

**Keywords:** multiple sclerosis; demyelination; optic neuritis; imaging; biomarkers

**Abbreviations:** IEAD = inter-eye absolute difference; IEPD = inter-eye percentage difference; mGCIPL = macular ganglion cell inner plexiform layer; MSON = multiple sclerosis associated optic neuritis; OCT = optical coherence tomography; pRNFL = peripapillary retinal nerve fibre layer

## Introduction

Multiple sclerosis is a disease that predominantly affects a young adult population in the prime of their working life. Accurate and early diagnosis of multiple sclerosis is important because of access to FDA-approved, effective disease-modifying treatments for a disease which affects more than 2 million individuals globally (Reich *et al.*, 2018). In the USA ~400 000 patients suffer from multiple sclerosis and the annual economic burden is ~\$10 billion (Reich *et al.*, 2018). There is a need to improve on the diagnostic work-up, incorporating technologies that are scalable to a population level in order to improve screening for this disabling condition. The last revision of the diagnostic criteria for multiple sclerosis highlighted the importance of interrogating the diagnostic value of retinal optical coherence tomography (OCT) for refinement of diagnostic criteria (Thompson *et al.*, 2018a; London *et al.*, 2019; Riederer *et al.*, 2019). Could inclusion of the optic nerve as a fifth CNS location for dissemination in space or time improve on the overall diagnostic sensitivity/specificity levels? Many multiple sclerosis lesions, including those of the optic nerve, are asymptomatic and detecting them earlier will permit for an earlier diagnosis (London *et al.*, 2019; Riederer *et al.*, 2019).

The rationale for considering OCT for the diagnostic work-up of patients stems from the high level of reproducibility of retinal layer atrophy measures from two systematic meta-analyses spanning two decades of work (Petzold *et al.*, 2010, 2017). The accuracy of the OCT data is such that the degree of peripapillary retinal nerve fibre layer (pRNFL) atrophy in eyes affected by multiple sclerosis associated optic neuritis (MSON) was almost identical in repeatability studies. A normal pRNFL has a global average thickness of ~100  $\mu\text{m}$ . Following MSON, time domain OCT data revealed atrophy of the pRNFL of 20.38  $\mu\text{m}$  [95% confidence interval (CI) 17.91–22.86  $\mu\text{m}$ ] (Petzold *et al.*, 2010). A decade later, spectral domain OCT data confirmed almost to the decimal point identical pRNFL atrophy values of 20.10  $\mu\text{m}$  (17.44–22.76  $\mu\text{m}$ ) (Petzold *et al.*, 2017). Optic nerve lesions are the main cause of retinal thinning across the spectrum of clinical multiple sclerosis phenotypes (Pulicken *et al.*, 2007; Costello *et al.*, 2009; Balk *et al.*, 2014). Longitudinal studies add weight to the argument that this is genuine pRNFL atrophy progressing at a rate of  $-0.36$  to  $-0.53$   $\mu\text{m}/\text{year}$  in optic neuritis in absence of multiple sclerosis (Petzold *et al.*, 2017). This is relevant because

MSON is a frequent presenting sign in multiple sclerosis and identified in 80% of patients post-mortem (Green *et al.*, 2010). Because of the asymmetry of pRNFL thickness between the two eyes following MSON, a consensus recommendation was to consider an inter-eye difference of  $>20\%$  (based on the 20- $\mu\text{m}$  difference from a ~100  $\mu\text{m}$  global average normal value) for the pRNFL as diagnostic evidence of an episode of MSON (Petzold *et al.*, 2014). A subsequent Dutch cohort analysis did, however, show that the original 20% estimate might be too conservative (Coric *et al.*, 2017). An inter-eye percentage difference (IEPD) of 9% for the pRNFL, but only 4% of the compound macular ganglion cell and inner plexiform layers (mGCIPL) distinguished between patients with MSON and healthy controls with high diagnostic accuracy and 9  $\mu\text{m}$  for the pRNFL inter-eye absolute difference (IEAD) (Coric *et al.*, 2017; Xu *et al.*, 2019). This finding has since been reproduced independently in two US cohorts (Nolan *et al.*, 2018; Xu *et al.*, 2019) and the international IMSVISUAL multi-centre study (Nolan-Kenney *et al.*, 2019). All four studies suggest that about a 4% (IEPD) or 4  $\mu\text{m}$  (IEAD) difference in the macula have a high diagnostic sensitivity.

Important limitations to these studies were the small number of controls with data on the GCIPL ( $n = 63$ ) (Coric *et al.*, 2017),  $n = 31$  (Nolan *et al.*, 2018), not specified (Xu *et al.*, 2019),  $n = 259$  (Nolan-Kenney *et al.*, 2019). All controls were healthy volunteers. This is an inclusion bias, which may limit the usefulness of the IEPD/IEAD in clinical practice where patients present with multiple diseases. None of the studies included data on the main public health problems known to affect OCT data such as diabetes mellitus, glaucoma and alcohol habits (Khawaja *et al.*, 2020). None of the studies presented data on key ophthalmological variables influencing OCT data such as intraocular pressure (IOP) and refraction (Khawaja *et al.*, 2020). Finally, most studies focused on MSON only rather than multiple sclerosis (Nolan *et al.*, 2018; Nolan-Kenney *et al.*, 2019; Xu *et al.*, 2019). However, asymmetry in the retinal thickness is also present in patients with optic neuritis in the absence of multiple sclerosis (Gabilondo *et al.*, 2013). Cumulatively, these shortcomings are limited in adequately informing how the IEPD/IEAD may contribute to future refinements of the diagnostic criteria in multiple sclerosis (Thompson *et al.*, 2018a).

We therefore conducted the present study using data from a large community cohort with rich phenotyping (Chua *et al.*, 2019). The main cause for asymmetric atrophy

of inner retinal layers is MSON (Nolan *et al.*, 2018; Nolan-Kenney *et al.*, 2019; Xu *et al.*, 2019). Therefore, patients with documented optic neuritis were excluded from the study. A smaller degree of atrophy can be attributed to damage to the retino-cortical projections (de Vries-Knoppert *et al.*, 2019). A pathologically frequent location of multiple sclerosis lesions is the periventricular white matter (Thompson *et al.*, 2018a), where the retino-cortical projections pass (Petzold *et al.*, 2010). Statistically the distribution of multiple sclerosis lesions is not symmetrical between the right and left hemisphere. The hypothesis tested is that there is a significant degree of retinal asymmetry in patients with multiple sclerosis, which can be quantified by the IEPD/IEAD (Coric *et al.*, 2017). In clinical practise, visual fields in patients with multiple sclerosis are never as homonymous as the idealized sketches shown in a textbook may suggest (Fujimoto and Adachi-Usami, 1998; Gündüz *et al.*, 1998; Lycke *et al.*, 2001). The reported asymmetry in the visual fields can also be observed anecdotally in the thickness maps of the macular OCT (see Figure 1 in Gabilondo *et al.*, 2013). There is always a degree of incongruity that is helpful to note for region of interest-based OCT analysis (de Vries-Knoppert *et al.*, 2019). Importantly, the robustness of the IEPD/IEAD as a complementary diagnostic test for multiple sclerosis was tested against a large list of co-morbidities, public health issues and ophthalmological variables.

## Materials and methods

### Study design and participants

UK Biobank is a community-based cohort of 502 656 UK residents aged 40–69 years and registered with the National Health Service (NHS). Examinations were carried out between 2007 and 2010 at 22 study assessment centres. The North West Multi-Centre Research Ethics Committee approved the study in accordance with the principles of the Declaration of Helsinki. The overall study protocol (<http://www.ukbiobank.ac.uk/resources/>) and protocols for individual tests (<http://biobank.ctsu.ox.ac.uk/crystal/docs.cgi>) are available online.

In brief, participants answered a wide-ranging touch-screen questionnaire covering demographic, socio-economic and lifestyle information, environmental exposures, and personal as well as family medical history. In 2009–10, additional examination components were added, including the eye examination. Visual acuity, autorefractometry/keratometry (Tomey RC5000), Goldmann-corrected IOP, (IOP<sub>g</sub>) and cornea-corrected IOP (IOP<sub>cc</sub>) (Ocular Response Analyzer, Reichert) were collected from 110 573 consecutive participants in 2009–10, and retinal OCT measurements were undertaken in 67 321 of these participants. The OCT protocol was described in detail (Patel *et al.*, 2016; Ko *et al.*, 2017) and is compliant with the APOSTEL guidelines (Cruz-Herranz *et al.*, 2016). In brief, high resolution spectral domain OCT imaging of undilated eyes was performed in a dark enclosed room using the Topcon 3D OCT 1000 Mk2 (Topcon Corp), on the same day as other physical measurements. We excluded OCT scans of poor imaging quality according to the OSCAR-IB criteria (Tewarie *et al.*, 2012). The R-

criterion was not used to permit for analyses of ocular co-morbidities. A flow chart of selection of participants is presented in Fig. 1.

### Ethical approval

The North West Multi-Centre Research Ethics Committee approved the study (reference no. 06/MRE08/65), in accordance with the tenets of the Declaration of Helsinki. Detailed information about the study is available at the UK Biobank website ([www.ukbiobank.ac.uk](http://www.ukbiobank.ac.uk)).

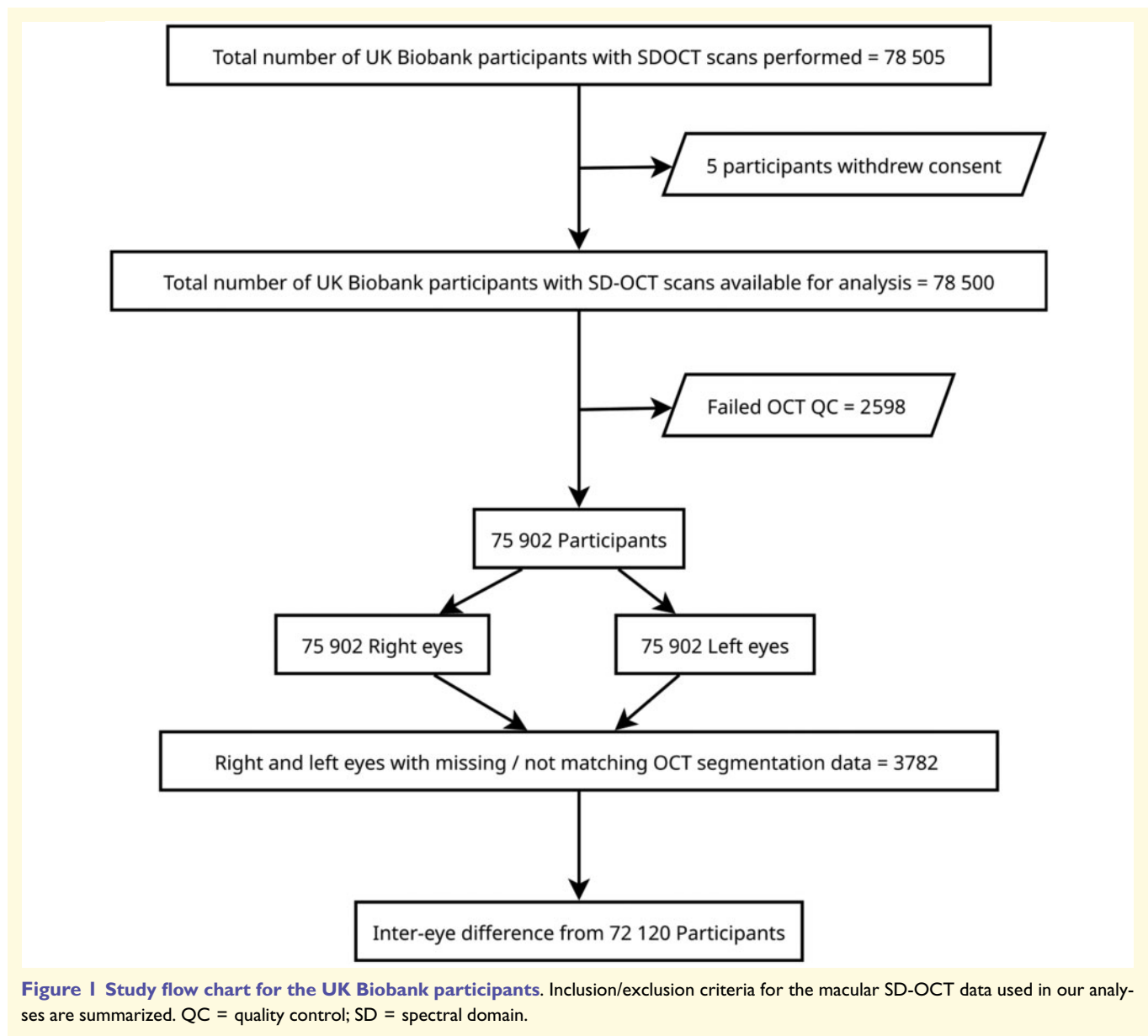
### Statistical analysis

Analyses followed EQUATOR Reporting Guidelines and were consistent with the STROBE outline for cohort studies (<https://www.equator-network.org/reporting-guidelines/>). The data used in this manuscript are from the UK Biobank Data Repository. The coding names for the variables used in this manuscript are spelled out for transparency. We used SAS version 9.4 (SAS Institute Inc., 100 SAS Campus Drive, Cary, NC 27513-2414, USA) for all analyses. Data distribution was checked by the Shapiro–Wilk test and visually. Normally distributed data are presented as mean and standard deviation (SD). The median and interquartile range are shown for non-Gaussian data. Categorical data are presented as number (percentage). As before, the quality assessment included exclusion of the top and bottom 1% percentile of the EDTRS grid-based measurements (Patel *et al.*, 2016). The inter-eye differences were calculated as described (Coric *et al.*, 2017; Nolan *et al.*, 2018). For each analysis we used both the IEPD (a dimensionless metric) and IEAD (in micrometres) from the ETDRS grid.

First, the diagnostic accuracy of the IEPD and IEAD were compared for inner retinal layer measurements used in previous studies. We adhered to the APOSTEL nomenclature (Cruz-Herranz *et al.*, 2016): the macular retinal nerve fibre layer (mRNFL), the macular ganglion inner plexiform layer (mGCIPL) and the composite of these two, the ganglion cell complex (mGCC). Performance of each of these measures was tested using receiver operator characteristics (ROC) curve analyses. Statistical comparison of ROC curves area under the curve (AUC) and 95% CI for the incremental contribution of each inter-eye measure was performed using the Wald test for the entire cohort (Seshan *et al.*, 2012). To maximize statistical power only the most statistically significant IEPD/IEAD measures were selected.

Second, patients were categorized in the main level 1, ICD-10 disease groups (clinician controlled). A total of  $n = 836$  diagnostic coding data fields (variables s\_41202\_0\_0 to s\_41205\_0\_11) were revised per patient. The ICD-10 code for multiple sclerosis G35 is applicable to all forms of multiple sclerosis, but does not specify which tests were used to reach a diagnosis. Patients with multiple sclerosis who also had optic neuritis documented were excluded. For ‘other eye diseases’ we pooled the ICD-10 categories H53, H54, H40, H42, H30, H31, H33, H34, H35, H36. This includes all forms of glaucoma, pathology of the vitreous body and globe, retina and choroid, other forms of visual disturbances and blindness, which can influence OCT measures.

Next, we calculated the cumulative disease burden per patient. For each disease group relevant variables known to influence OCT data were included: age (variable n\_21003\_0\_0), gender (n\_31\_0\_0), ethnicity (n\_21000\_0\_0), the body mass



index (BMI, n\_23104\_0\_0), smoking habits (n\_20160\_0\_0) and alcohol consumption in previous 24 h (n\_100022\_0\_0). For the diabetes mellitus status (type I and type II), ICD-10 coding was double-checked with field (n\_2443\_0\_0). Likewise, we included for each eye: logMAR visual acuities [OD (right eye) = n\_5206\_0\_0, OS (left eye) = n\_5208\_0\_0], refraction in dioptres (dpt, OD = n\_5084\_0\_0, OS = n\_5085\_0\_0), refraction based anisometropia (> 1 dpt), and IOP (OD = n\_5262\_0\_0, OS = n\_5262\_1\_0).

We used ROC curve analyses for comparing patients with multiple sclerosis to control subjects and different combinations of disease groups. The diagnostic value was rated as good for an AUC > 0.7 (Coric *et al.*, 2017; Nolan-Kenney *et al.*, 2019). Cut-off points for sensitivity/specificity levels were determined graphically and calculated with the Youden index (Coric *et al.*, 2017; Nolan-Kenney *et al.*, 2019). Univariate and multivariable analyses were performed using odds ratios (OR) to adjust for

potential confounders (Lingsma *et al.*, 2010). The OR also permit to estimate of the effect sizes for categorical variables (for example, diabetes mellitus yes/no). To complement the statistical comparisons of continuous variables we also calculated effect sizes for a within-subjects variability. We used the partial  $\omega^2$  and its standard deviation (alpha = 0.1). This is because for future power analyses and sample size calculations the  $\omega^2$  has less of a bias than  $\theta^2$ , which generally suggests a larger effect size (Albers and Lakens, 2018). The effect size is reported as very small for  $\omega^2$  0–0.01; small for  $\omega^2$  0.01–0.06; medium for  $\omega^2$  0.06–0.14 and large for  $\omega^2$  > 0.14. For the forest plot, logistic regression was fitted including the multiple sclerosis status as the dependent variable and the mGCIPL, IEPD, and IEAD as the predictors. We did not impute data. We provided the exact number of data-points for each analysis and variable in order to account for missing observations. The null hypothesis was rejected if  $P < 0.05$ .

## Data availability

The corresponding author can provide the dataset used or documentation on the analysis performed upon reasonable request. The data can also be downloaded directly from the UK Biobank (<http://www.ukbiobank.ac.uk>).

## Results

Between 2009 and 2010, 78 505 individuals underwent OCT imaging. Of these, 72 120 had matching high quality OCT imaging from both eyes permitting calculation of the inter-eye differences (Fig. 1). The prevalence of multiple sclerosis (ICD-10 coding) in the cohort was 168/74 568 (0.23%). After exclusion of optic neuritis there remained 71 939 control subjects and 144 patients with multiple sclerosis (Table 1).

The diagnostic accuracy of the inter-eye differences for mRNFL, mGCIPL and mGCC were determined by ROC (AUC, 95% CI, Table 2). The highest AUC was achieved for the inter-eye differences from the mGCIPL. The discriminative performance of IEPD (mGCIPL) and IEAD (mGCIPL) were significantly better than for the mRNFL and mGCC (Table 2). The IEPD (mGCIPL) had a marginally better discriminatory power than the IEAD for all retinal layers. The inter-eye differences for the mRNFL were of no or low discriminatory power. The IEPD and IEAD for the mGCIPL were selected for further comparisons.

Figure 2A illustrates that the number of co-morbidities is relevant. The highest discriminatory power is achieved for the IEPD (AUC 0.74) and IEAD (AUC 0.73) for separating patients with multiple sclerosis from healthy controls. The

diagnostic discriminatory power of the IEPD and IEAD for multiple sclerosis is reduced if the number of co-morbidities increases from zero in healthy control subjects to between one to four co-existing disease categories (Fig. 2A). Thereafter the IEPD and IEAD become poor (AUC < 0.7). Both tests are near useless if more than nine co-morbidities co-exist.

Figure 2B illustrates that the good discriminatory power (AUC > 0.7) of the IEPD and IEAD are also influenced by individual groups of diseases. The IEPD (mGCIPL) performs consistently better than the IEAD for 15 of 15 group comparisons. Detailed demographic data and description of potential confounders are presented in Supplementary Table 1.

The results of the univariate and multivariable analyses are summarized in Fig. 3A and B. As detailed in the 'Materials and methods' section, the results of the multivariate analyses were shown for each of the dichotomized demographic and clinical variables. For each subgroup in the forest plot, the number of patients that entered the analyses is given.

Taken together, in Fig. 3 the ORs were highly significant for making a diagnosis of multiple sclerosis for the IEPD (OR 1.13, 95%CI 1.1–1.16,  $P < 0.0001$ , Fig. 3A) and the IEAD (OR 1.16, 95%CI 1.13–1.2,  $P < 0.0001$ , Fig. 3B) compared to the control cohorts (Table 1). Both measures retained their level of significance for making a diagnosis of multiple sclerosis for a whole range of covariates. Significance was, however, lost for four covariates (highlighted in red in Fig. 3A and B). These were higher age (>65 years), a non-white ethnic background, presence of other eye conditions, or diabetes mellitus. Significance of the OR was not affected by ocular covariates: visual acuity, IOP or need for refraction.

Table 3 summarizes the effect size calculations for the mGCIPL IEPD and IEAD to distinguish patients with multiple sclerosis from the control subjects. The IEPD has a small effect size ( $\omega^2$  0.0376) with a small CI (0.0108). The IEAD has larger effect size ( $\omega^2$  0.3325) and CI (0.024). For the IEPD, effect sizes always increase through interaction. For the IEAD, only the interaction with visual acuity

**Table 1 Subject characteristics and OCT data used in this study**

	All controls	Multiple sclerosis
<i>n</i>	71 939	144
Age, years	56.67 ± 8.05	55.20 ± 7.82
Female sex (%)	38 633 (54)	110 (74)
Optic neuritis (%)	0 (0%)	0 (0)
mRNFL OD, $\mu\text{m}$	30.38 ± 6.42	26.84 ± 7.02
mRNFL OS, $\mu\text{m}$	28.04 ± 6.01	25.32 ± 7.12
IEPD mRNFL, %	13.35 ± 12.54	17.13 ± 15.08
IEAD mRNFL, $\mu\text{m}$	0.60 ± 6.92	2.44 ± 7.42
mGCIPL OD, $\mu\text{m}$	72.36 ± 6.28	67.21 ± 7.04
mGCIPL OS, $\mu\text{m}$	72.45 ± 6.23	67.65 ± 7.05
IEPD mGCIPL, %	2.76 ± 3.56	6.51 ± 6.23
IEAD mGCIPL, $\mu\text{m}$	2.03 ± 2.63	4.62 ± 4.62
mGCC OD, $\mu\text{m}$	102.74 ± 9.65	94.05 ± 12.12
mGCC OS, $\mu\text{m}$	100.49 ± 9.13	92.97 ± 11.78
IEPD mGCC, %	2.40 ± 7.40	6.90 ± 9.69
IEAD mGCC, $\mu\text{m}$	2.63 ± 7.97	7.06 ± 10.17

The pooled data for all control subjects are shown next to the data for people suffering from multiple sclerosis. The mean ± standard deviation and numbers (percentage) are shown. mGCC = macular ganglion cell complex; mRNFL = macular retinal nerve fibre layer; OD = right eye; OS = left eye.

**Table 2 The inter-eye differences of the mRNFL, mGCIPL and mGCC**

Inter-eye difference	AUC	95% CI	P-value	P-value
IEPD mGCIPL	0.7110	0.6646–0.7575	Reference	0.318
IEAD mGCIPL	0.7075	0.6621–0.7529	0.318	Reference
IEPD mGCC	0.6483	0.5979–0.6987	0.0073	0.011
IEAD mGCC	0.6419	0.5925–0.6912	0.003	0.0043
IEPD mRNFL	0.5948	0.5451–0.6445	<0.0001	<0.0001
IEAD mRNFL	0.5859	0.5383–0.6334	<0.0001	<0.0001

Both the absolute (IEAD) and percentage (IEPD) differences are presented for separating patients with multiple sclerosis from the pooled cohort of UK Biobank subjects (Table 1). The ROC AUC, 95% Wald CI are shown. For each measure the ROC of the IEPD mGCIPL and IEAD mGCIPL are compared as reference to the other ROC curve analyses (AUC). mGCC = macular ganglion cell complex; mRNFL = macular retinal nerve fibre layer.

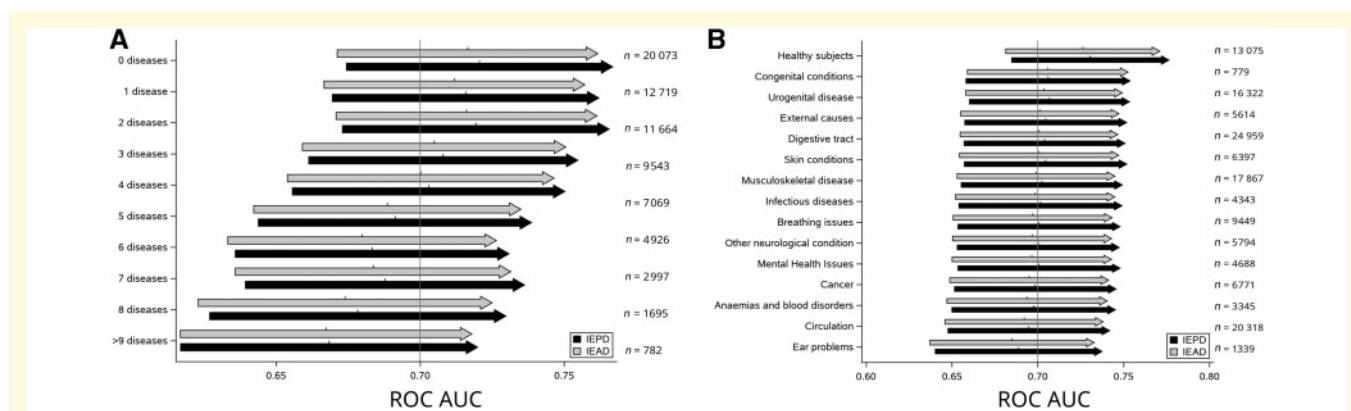


**Figure 2** The usefulness of the mGCIPL IEPD and IEAD as a paraclinical test for multiple sclerosis. The graph shows group comparisons. The reference group are patients suffering from multiple sclerosis. The other groups are composed of participants with a range of other diseases. Because patients can have more than one disease, they could be included in more than one group in this analysis. We analysed both the number of diseases co-existing in patients and the type of disease. All analyses were based on statistical comparisons of the AUC between different ROCs (see also [Supplementary Fig. 1](#)). **(A)** The impact of the number of co-morbidities is illustrated. The more diseases co-exist in patients, the less useful the IEPD and IEAD become as a diagnostic test for multiple sclerosis. For all comparisons, the IEPD (black bars) performs better than the IEAD (grey bars). **(B)** The influence of other disease groups (ICD-10) on making the diagnosis of multiple sclerosis. The best results are achieved for the conditions listed on the top of the graph (control subjects). The test is clinically useful if located to the right of the vertical reference line ( $>0.7$ ). This is the case for horizontal bars where the small vertical tick (ROC AUC value, indicated by arrow) on top of the horizontal bar (95% CI) is located to the right of the vertical reference line. [Supplementary Fig. 1](#) illustrates this step in more detail. The patient numbers per group for the comparison to patients with multiple sclerosis ( $n = 144$ ) are presented to the right of the bar chart and respective demographic data are summarized in [Supplementary Table 1](#).

increases the effect size. For all other interactions, the effect size decreases to become non-significant for alcohol.

The diagnostic sensitivity and specificity levels were calculated for the entire pooled control cohort ([Table 1](#)). Based on the previously published cut-off levels ([Coric et al., 2017](#); [Nolan-Kenney et al., 2019](#)) for the IEPD (mGCIPL, 4%) and IEAD (mGCIPL, 4  $\mu$ m), the sensitivities were 51.7% and 43.5%, respectively. Specificity levels were 82.8% and 86.8%. The positive predictive values were 0.6% and 0.7%. The negative predictive values were 99.9% and 99.9% ([Table 4](#)).

## Subgroup analysis

The cohort description for patients with neuromyelitis spectrum disorder is presented in [Supplementary Table 3](#). The corresponding sensitivity, specificity, positive predictive and negative predictive values in this context were poor ([Table 5](#)).

## Discussion

The main finding of this study was that the previously published inter-eye difference of mGCIPL is specific ( $\sim 82$ – $87\%$ ), but not sensitive ( $\sim 44$ – $52\%$ ) for identifying multiple sclerosis in a large cohort drawn from UK communities. Most specifically, this applies to the IEPD (mGCIPL) and IEAD (mGCIPL). For the first time, evidence is provided that there are relevant co-variables that influence the discriminatory power of both measures. These are age over 65 years, a non-white ethnic background, presence of

eye pathologies and presence of diabetes mellitus. This is also the first study to test the value of OCT for contributing to a diagnosis of multiple sclerosis not only in comparison with control subjects ([Petzold et al., 2010, 2017](#)), but also compared to other diseases. There is a stepwise decrease of the discriminatory power of the IEPD/IEAD with increasing number of co-morbidities. The predominance of participants of white ethnic background and a slight female excess in our study is consistent with the epidemiology of multiple sclerosis ([Thompson et al., 2018b](#)). The prevalence of multiple sclerosis in this study, 0.0020 (95%CI 0.0023–0.0031), was within the expected range for the UK of 100 to 300:100 000 ( $=0.003$ ) ([Thompson et al., 2018b](#)). The study is therefore in line with expected prevalence of disease and an inclusion bias is unlikely.

Previous studies on IEAD only assessed the value of making a diagnosis of unilateral MSON, but not system-wide multiple sclerosis *per se* ([Nolan et al., 2018](#); [Nolan-Kenney et al., 2019](#); [Xu et al., 2019](#)). For the IEPD, [Coric et al. \(2017\)](#) reported an AUC of 0.77 for multiple sclerosis if compared to healthy controls. The present data confirm that this observation also holds for a community sample including a broad range of pathologies with a ROC AUC of 0.71 (95%CI 0.67–0.76).

The best AUCs for the mGCIPL were reported for unilateral MSON ([Coric et al., 2017](#); [Nolan et al., 2018](#); [Nolan-Kenney et al., 2019](#)). The AUC decreased from 0.91 (IEPD) in a single-centre study ([Coric et al., 2017](#)) to 0.79 (IEAD) in a US multi-centre study ([Nolan et al., 2018](#)), to 0.77 (IEAD) in an international multi-centre study ([Nolan-](#)

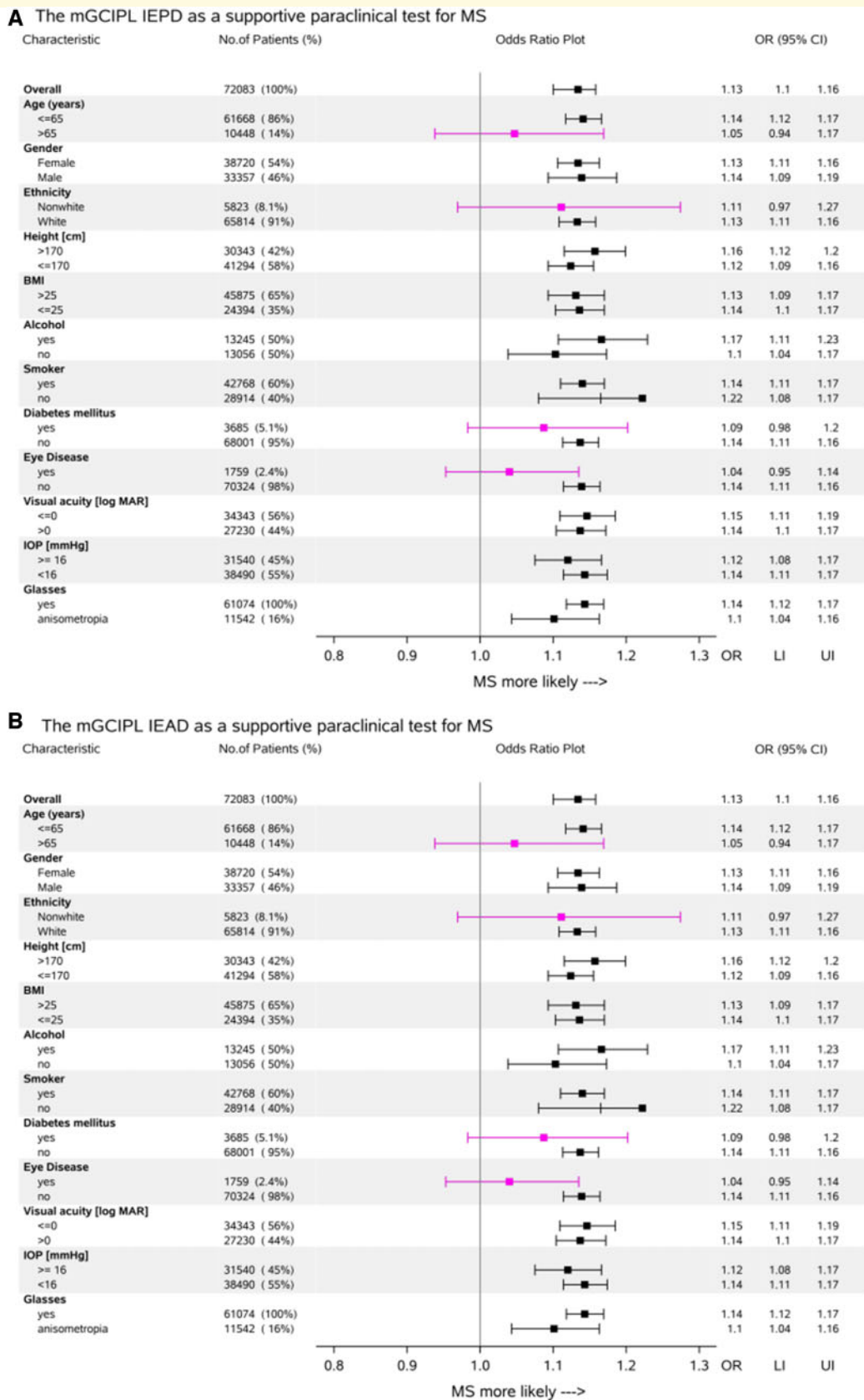


**Figure 3** Univariable and multivariable analysis of the IEPD and IEAD as a supportive test for multiple sclerosis. The graph shows the group comparison between people suffering from multiple sclerosis and the control group from Table 3. (A) In the univariate analysis the IEPD provides a robust supportive diagnostic test for multiple sclerosis (OR 1.11) with narrow 95% CI (1.09–1.13). The multivariable analyses show that significance is retained for all but three combinations, highlighted in red (IEPD at age > 65 years, IEPD in non-white subjects, IEPD in patients with diabetes mellitus). (B) The IEAD has very similar properties in the univariate and multivariable analyses with higher age, non-white ethnicity and diabetes mellitus being relevant covariates.

**Table 3** Effect sizes of the mGCIPL IEPD and IEAD for separating patients with multiple sclerosis from control subjects

OCT	Interaction	$\omega^2$	LI	UI	Effect size
IEPD	–	0.0223	0.0182	0.0268	Small
IEPD	IOP	0.3655	0.3498	0.3808	Large
IEPD	Refraction	0.3111	0.2934	0.3283	Large
IEPD	BMI	0.2981	0.2862	0.3099	Large
IEPD	VA	0.2340	0.2220	0.2460	Large
IEPD	Height	0.1505	0.1403	0.1609	Large
IEPD	Alcohol	0.1984	0.0897	0.1059	Large
IEPD	Age	0.0976	0.0892	0.1063	Medium
IEAD	–	0.0496	0.0467	0.0525	Small
IEAD	VA	0.3419	0.3172	0.3656	Large
IEAD	IOP	0.2896	0.1789	0.3797	Large
IEAD	Refraction	0.2504	0.1391	0.3422	Large
IEAD	BMI	0.2198	0.1788	0.2580	Large
IEAD	Age	0.1876	0.1698	0.2051	Large
IEAD	Height	0.0971	0.0727	0.1210	Medium
IEAD	Alcohol	–0.0850	0	0	NS

The partial  $\omega^2$  values are shown for the IEPD and IEAD alone (no interaction is indicated with a dash) and continuous variables. Interactions are sorted in descending according to the effect size. BMI = body mass index; IOP = intraocular pressure; NS = not significant; VA = visual acuity.

Kenney *et al.*, 2019). This is marginally better than the AUC of 0.73 for the IEAD comparing patients with system-wide multiple sclerosis to control subjects without co-morbidities (Fig. 2A) in the present study. We assume that this difference in performance of the IEPD and IEAD from previous studies results from inclusion of younger participants with fewer co-morbidities, which would inflate the discriminative power of the test. In the Nolan *et al.* (2018) study, control patients were 35.3 years of age compared to 40.6 years for patients with MSON. This is relevant because present data reveal age to be a relevant covariate (Fig. 3). Therefore, our reported AUC of 0.73–0.74 for both the IEPD and IEAD in age-matched patients with multiple sclerosis and control subjects is more representative.

It is important to highlight the relevance that an inclusion bias can have on the potential over-interpretation of the diagnostic value of a new test. Clearly, Fig. 2 illustrates that the highest discriminatory power for the inter-eye differences is found in comparison of control subjects without co-morbidities with patients who suffer from multiple sclerosis. In the presence of any other disease, the discriminatory power of the inter-eye differences drops. This was also shown in the subgroup analysis for NMOSD. Likewise, presence of multiple co-morbidities severely limits the value of the IEPD and IEAD as a diagnostic test for multiple sclerosis.

Consistent with previous reports, the retinal layer with the highest discriminatory power is the mGCIPL. This is reassuring because it is in line with multi-centre studies assessing the accuracy of individual retinal layer segmentation (Oberwahrenbrock *et al.*, 2018). We discourage the use of the mRNFL as a measure in this context because of the

much higher likelihood of automated segmentation error due to the presence of common ocular disorders such as epiretinal membrane, among many other causes (Tewarie *et al.*, 2012; Oberwahrenbrock *et al.*, 2018).

Importantly, some of the exclusion criteria previously listed, such as refraction of  $>5$  dpt (Tewarie *et al.*, 2012) were not found to be relevant for the discriminatory power of the IEPD/IEAD. This can be explained by relative symmetric effects of myopia and hypermetropia on both eyes in the same subject (Cameron *et al.*, 2017). The inter-eye difference is not affected by this, but the individual absolute retinal layer thickness values are. Therefore, the present data suggest that the IEPD/IEAD may also be of diagnostic value in patients across a range of refractive errors. Anticipating even more detailed future retinal imaging capabilities, we note that there will be no perfect symmetry in healthy control subjects because a small degree of asymmetry between eyes is part of nature's strategy to optimize processing of sensory input (Cameron *et al.*, 2017).

A key challenge in making a diagnosis of multiple sclerosis is the lack of test specificity. For example, it has been shown that the diagnostic specificity of MRI brain scans for multiple sclerosis was only 29% using the American Academy of Neurology criteria if compared to MRI brain scans from patients with other neurological diseases (Nielsen *et al.*, 2005). Inclusion of spinal MRI scans and updated diagnostic criteria over the past decade have since improved diagnostic sensitivity and specificity (Filippi *et al.*, 2016, 2018; Thompson *et al.*, 2018a). For optic neuritis 3D-double inversion recovery (DIR) is of high sensitivity (London *et al.*, 2019; Davion *et al.*, 2020). But even cutting edge MRI criteria using the central vein sign are dependent on optimization of cut-off level sensitivities for diagnosing multiple sclerosis against other diseases as low as 2.0% to reach a 100% specificity level (Sinnecker *et al.*, 2019). In the same study the highest sensitivity levels reached were 89.7%, with specificities down to 54.9% (Sinnecker *et al.*, 2019).

Likewise there are limitations to the use of visual evoked potentials (VEPs), which can give false positive results in a whole range of conditions (Petzold *et al.*, 2014). The need for rigorous standardization of electrodiagnostic assessments, incorporating an electroretinogram, has been noted (Odom *et al.*, 2016), but is not systematically done. Finally, the diagnostic specificity for multiple sclerosis drops for CSF oligoclonal bands from 94% in healthy controls to only 61% in patients with other inflammatory conditions (Petzold, 2013). In this context, the low diagnostic specificities of the OCT metrics on previously published cut-off levels (Coric *et al.*, 2017; Nolan-Kenney *et al.*, 2019) IEPD (mGCIPL, 82.8%) and IEAD (mGCIPL, 86.8%) are not incongruous. But the effect sizes if used in isolation ( $\omega^2$ , see Table 3) and the low OR emphasize the need to improve the performance of the IEPD and IEAD further.

An important question, which this study cannot answer, is if retinal OCT is superior to other tests in (i) detecting asymptomatic optic nerve involvement; and (ii) monitoring progression of neurodegeneration longitudinally. This point



**Table 4** The sensitivity, specificity, positive predictive value (PPV) and negative predictive value (NPV) for the mGCIPL IEPD and IEAD as a supportive diagnostic test for multiple sclerosis

mGCIPL	Cut-off	References	Specificity	Sensitivity	PPV	NPV
IEPD	20 %	Petzold <i>et al.</i> , 2014	99.4	2.7	0.998	0.01
IEPD	4 %	Coric <i>et al.</i> , 2017	82.8	51.7	0.6	99.9
IEAD	4 $\mu$ m	Nolan-Kenney <i>et al.</i> , 2019	86.8	43.5	0.7	99.9

The levels were calculated for the published cut-off levels for the Heidelberg Spectralis OCT (Petzold *et al.*, 2014; Coric *et al.*, 2017; Nolan-Kenney *et al.*, 2019). All values presented in the table were calculated from the comparison of patients with multiple sclerosis to all controls (as summarized in Table 1).

The IEPD/IEAD qualifies as a supportive test for diagnostic criteria, but would not yet be sustainable as a screening test on a population level.

**Table 5** Subgroup analysis multiple sclerosis compared to NMSOD

mGCIPL	Cut-off	References	Specificity	Sensitivity	PPV	NPV
IEPD	20 %	Petzold <i>et al.</i> , 2014	2.7	100	29.2	100
IEPD	4 %	Coric <i>et al.</i> , 2017	72.8	51.7	82.6	37.7
IEAD	4 $\mu$ m	Nolan-Kenney <i>et al.</i> , 2019	76.3	43.5	35.2	82.1

All values presented in the table were calculated from the comparison of patients with multiple sclerosis to patients with NMSOD (as summarized in Supplementary Table 1). NPV = negative predictive value; PPV = positive predictive value.

is relevant because of the likelihood that asymptomatic optic nerve/tract/radiation involvement contributed to the retinal asymmetry findings.

Other limitations of our study include that we have not studied specific subtypes of multiple sclerosis, particularly a well-defined clinically isolated syndrome cohort with simultaneous recording of VEP may be of future interest. Likewise, we do not have long-term follow-up data on clinical scales, disability progression and MRI metrics as in previous studies (Coric *et al.*, 2017; Nolan-Kenney *et al.*, 2019; Xu *et al.*, 2019). Patients with multiple sclerosis were relatively old because of the UK Biobank age inclusion criteria (Chua *et al.*, 2019). We did, however, have data on presence or absence of optic neuritis in other conditions and these data are listed in Table 3. But we do not know how long ago an episode of optic neuritis prior to the OCT was. It is very likely that the incidence of optic neuritis, known to be ~40–80% multiple sclerosis, is under-reported in the UK Biobank, at only 2%. We do not know about disease duration or the treatment history with disease-modifying treatments. The granularity of data to answer these questions will come from smaller sized multiple sclerosis cohort studies. It can therefore not be excluded that better sensitivity and specificity levels may be reached with deeper phenotyping including the recognition of small, asymptomatic multiple sclerosis lesions, which included asymptomatic optic neuritis (London *et al.*, 2019; Davion *et al.*, 2020). Recognizing these shortcomings, there are strengths to this study as well. One is that the examination of ophthalmological problems has been carried out in far greater detail, particular with regard to IOP and glaucoma, than any of the OCT studies in multiple sclerosis (Petzold *et al.*, 2010, 2017). The UK Biobank did not include imaging of the optic disc and we are therefore unable to comment on the pRNFL. Likewise, the problem of systemic co-morbidities in patients with multiple sclerosis has—to the best of our

knowledge—not been addressed in any of the previous OCT studies in multiple sclerosis. On balance, this community-based study offers certain advantages that add valuable data to the literature.

Whilst this study was under review, three more studies on the inter-eye difference of the GCIPL have been published (Behbehani *et al.*, 2020; Davion *et al.*, 2020; Outteryck *et al.*, 2020; Villoslada *et al.*, 2020). Taken together, these studies are in line with present data. If compared to a healthy control group the inter-eye GCIPL difference gives near perfect sensitivity (100%) and specificity (98%) values (Behbehani *et al.*, 2020). Separating MRI confirmed symptomatic from asymptomatic lesions, optimized inter-eye GCIPL differences gave sensitivity levels of 88.2% and 89.3%, respectively (Outteryck *et al.*, 2020). The corresponding specificity levels were 83.3% and 72.6%. But if comparisons are made with diseased, even if asymptomatic, control subjects' sensitivity drops to 67.3% with a specificity of 67.4% (Davion *et al.*, 2020).

It is likely that the use of artificial intelligence (AI)-based approaches, notably deep learning, will further improve on the diagnostic value of retinal OCT data in multiple sclerosis, similar to what has been achieved for retinal diseases (Fauw *et al.*, 2018). Such an AI approach should be guided by the insights on 'pattern recognition', which led to the present study. First, reliable retinal layer segmentation on high quality scans and second, use of inter-eye differences rather than single eye measurements. The use of a region of interest-based OCT approach (de Vries-Knoppert *et al.*, 2019) should be investigated in order to optimize detection of retinal asymmetry visible in individual cases (Gabilondo *et al.*, 2013). This extends on our introductory remark on the known incongruous appearance of visual field defects in multiple sclerosis (Fujimoto and Adachi-Usami, 1998; Gündüz *et al.*, 1998; Lycke *et al.*, 2001). Expanding on this, there may be an additional role for outer retinal layers

(Saidha *et al.*, 2011) and assessment of the retinal vasculature (Kleerekooper *et al.*, 2020). Further improvement may come from quantification of atrophy progression over time (Aly *et al.*, 2020). For such future AI-based studies, additional statistical requirements will need to be met, including cross-validation of cut-off values. The UK Biobank and a global collaborative initiative, IMSVISUAL (<http://www.imsvisual.org>) provide OCT datasets ideally suited for training and validation of such future algorithms.

Taken together, previous studies (Coric *et al.*, 2017; Nolan-Kenney *et al.*, 2019; Xu *et al.*, 2019; Behbehani *et al.*, 2020; Davion *et al.*, 2020) left at least three open questions. First, how do IEPD and IEAD perform when used in a large community, including some individuals with other pathologies, rather than ‘hyper-normal’ controls? An important conclusion from this study is that the much smaller cut-off values compared to earlier studies will demand a rigorous handling of OCT quality control criteria in clinical practise. Even small artefacts by poor OCT technique can mask the small difference observed. Second, is there an advantage in applying either the IEPD or IEAD? And third, do IEPD/IEAD also have a diagnostic role in generalized multiple sclerosis rather than only MSON? We made use of cross-sectional data in a large community cohort study to address these three questions. The challenge is open for AI-based analyses of retinal asymmetry in multiple sclerosis to improve sensitivity and specificity levels. We conclude that presently, the IEPD and IEAD can both be recommended for consideration as an additional supportive paraclinical test in young subjects with less than five co-morbidities for future revisions of multiple sclerosis diagnostic criteria.

## Funding

This analysis was supported by the Eranda Foundation via the International Glaucoma Association, UCL ORS & GRS programmes. A.P., N.G.S., P.T.K., P.J.F., and P.J.P. received salary support from the NIHR BRC at Moorfields Eye Hospital. The authors acknowledge a proportion of our financial support from the UK Department of Health through an award made by the National Institute for Health Research to Moorfields Eye Hospital NHS Foundation Trust and UCL Institute of Ophthalmology for a Biomedical Research Centre for Ophthalmology. P.T.K. is supported in part by the Helen Hamlyn Trust. P.J.F. received support from the Richard Desmond Charitable Trust, via Fight for Sight, London. P.A.K. is supported by a Clinician Scientist award (CS-2014-14-023) from the National Institute for Health Research. The views expressed in this publication are those of the author(s) and not necessarily those of the NHS, the National Institute for Health Research or the Department of Health. The UK Biobank Eye and Vision Consortium is supported by grants from Moorfields Eye Charity, The NIHR Biomedical Research Centre at Moorfields Eye Hospital NHS Foundation Trust and UCL Institute of Ophthalmology and the Alcon Research

Institute. The NIHR BRC at Moorfields Eye Hospital supported A.P., N.G.S., P.A.K., P.T.K., P.J.F., and P.J.P. This analysis was supported by the Eranda Foundation via the International Glaucoma Association, UCL ORS and GRS programmes. P.J.F. received support from the Richard Desmond Charitable Trust, via Fight for Sight, London.

## Competing interests

A.P. reports personal fees from Novartis, Heidelberg Engineering, Zeiss, grants from Novartis, outside the submitted work; and A.P. is part of the steering committee of the OCTiMS study which is sponsored by Novartis. A.P. is part of the steering committee of Angio-OCT which is sponsored by Zeiss. He does not receive honorary as part of these activities. P.A.K. reports personal fees from Allergan, personal fees from Topcon, personal fees from Heidelberg Engineering, personal fees from Haag-Streit, personal fees from Novartis, personal fees from Bayer, personal fees from Optos, personal fees from DeepMind, grants from National Institute for Health Research (NIHR), outside the submitted work. C.R. reports employment by Topcon Healthcare Solutions Inc., outside submitted work. N.G.S. has nothing to disclose. P.J.F. reports personal fees from Allergan, Carl Zeiss, Google/DeepMind and Santen, a grant from Alcon, outside the submitted work. J.P. reports grants from Topcon Inc, outside the submitted work.

## Supplementary material

Supplementary material is available at *Brain* online.

## Appendix I

The UK Biobank Eye and Vision Consortium consists of the following members: Denize Atan, PhD; Tariq Aslam, PhD; Sarah A. Barman, PhD; Jenny H. Barrett, PhD; Paul Bishop, PhD; Catey Bunce; Roxana O. Carare, PhD; Usha Chakravarthy, FRCOphth; Michelle Chan, FRCOphth; Sharon Y.L. Chua, PhD; David P. Crabb, PhD; Alexander Day, FRCOphth, PhD; Parul Desai, FRCOphth, PhD; Bal Dhillon, FRCOphth; Andrew D. Dick, FMedSci, FRCOphth; Cathy Egan; Sarah Ennis, PhD; Paul J Foster, FRCS(Ed), PhD; Marcus Fruttiger, PhD; John E.J. Gallacher, MSc, PhD; David F. Garway-Heath MD(Res), FRCOphth; Jane Gibson, PhD; Dan Gore, FRCOphth; Jeremy A. Guggenheim, PhD; Chris J. Hammond, FRCOphth; Alison Hardcastle, PhD; Simon P. Harding, MD; Ruth E. Hogg; Pirro Hysi, PhD; Pearse A. Keane, MD; Sir Peng T. Khaw, PhD; Anthony P. Khawaja, DPhil; Gerassimos Lascaratos, PhD; Andrew J. Lotery, MD; Tom Macgillivray, PhD; Sarah Mackie, PhD; Michelle McGaughey; Bernadette McGuinness, PhD; Gareth J. McKay, PhD; Martin McKibbin, FRCOphth; Tony Moore,

FRCOphth; James E. Morgan; Zaynah A. Muthy, BSc; Eoin O'Sullivan, MD; Chris G. Owen, PhD; Praveen Patel, MD(Res), FRCOphth; Euan Paterson, BSc; Tunde Peto, PhD; Axel Petzold, PhD FRCP; Jugnoo S. Rahi, FRCOphth; Alicja R. Rudnicka, PhD; Jay Self, PhD; Sobha Sivaprasad, FRCOphth; David Steel, FRCOphth; Irene Stratton, MSc; Nicholas Strouthidis, PhD; Cathie Sudlow, DPhil; Dhanes Thomas, FRCOphth; Emanuele Trucco, PhD; Adnan Tufail, FRCOphth; Veronique Vitart, PhD; Stephen A. Vernon, DM; Ananth C. Viswanathan, PhD, FRCOphth; Cathy Williams, PhD; Katie Williams, PhD; Jayne V. Woodside, MRCOphth; Max M. Yates, PhD; and Yalin Zheng, PhD.

Please refer to the [Supplementary material](#) for member affiliations.

## References

- Albers C, Lakens D. When power analyses based on pilot data are biased: inaccurate effect size estimators and follow-up bias. *J Exp Soc Psychol* 2018; 74: 187–95.
- Aly L, Havla J, Lepenietier G, Andlauer TFM, Sie C, Strauß E-M, et al. Inner retinal layer thinning in radiologically isolated syndrome predicts conversion to multiple sclerosis. *Eur J Neurol* 2020. doi: 10.1111/ene.14416.
- Balk L, Tewarie P, Killestein J, Polman C, Uitdehaag B, Petzold A. Disease course heterogeneity and OCT in multiple sclerosis. *Mult Scler* 2014; 20: 1198–206.
- Behbehani R, Ali A, Al-Omairah H, Rouseff RT. Optimization of spectral domain optical coherence tomography and visual evoked potentials to identify unilateral optic neuritis. *Mult Scler Relat Disord* 2020; 41: 101988.
- Cameron JR, Megaw RD, Tatham AJ, McGrory S, MacGillivray TJ, Doubal FN, et al. Lateral thinking - Interocular symmetry and asymmetry in neurovascular patterning, in health and disease. *Prog Retin Eye Res* 2017; 59: 131–57.
- Chua SYL, Thomas D, Allen N, Lotery A, Desai P, Patel P, et al. Cohort profile: design and methods in the eye and vision consortium of UK Biobank. *BMJ Open* 2019; 9: e025077.
- Coric D, Balk LJ, Uitdehaag BMJ, Petzold A. Diagnostic accuracy of optical coherence tomography Inter-Eye Percentage Difference (IEPD) for optic neuritis in multiple sclerosis. *Eur J Neurol* 2017; 24: 1479–84.
- Costello F, Hodge W, Pan YI, Freedman M, DeMeulemeester C. Differences in retinal nerve fiber layer atrophy between multiple sclerosis subtypes. *J Neurol Sci* 2009; 281: 74–9.
- Cruz-Herranz A, Balk LJ, Oberwahrenbrock T, Saidha S, Martinez-Lapiscina EH, Lagreze WA, et al. The APOSTEL recommendations for reporting quantitative optical coherence tomography studies. *Neurology* 2016; 86: 2303–9.
- Davion J-B, Lopes R, Drumez É, Labreuche J, Hadhoum N, Lannoy J, et al. Asymptomatic optic nerve lesions: an underestimated cause of silent retinal atrophy in multiple sclerosis. *Neurology* 2020.
- Fauw JD, Ledsam JR, Romera-Paredes B, Nikolov S, Tomasev N, Blackwell S, et al. Clinically applicable deep learning for diagnosis and referral in retinal disease. *Nat Med* 2018; 24: 1342–50.
- Filippi M, Preziosa P, Meani A, Ciccarelli O, Mesaros S, Rovira A, et al. Prediction of a multiple sclerosis diagnosis in patients with clinically isolated syndrome using the 2016 MAGNIMS and 2010 McDonald criteria: a retrospective study. *Lancet Neurol* 2018; 17: 133–42.
- Filippi M, Rocca MA, Ciccarelli O, De Stefano N, Evangelou N, Kappos L, et al. MRI criteria for the diagnosis of multiple sclerosis: MAGNIMS consensus guidelines. *Lancet Neurol* 2016; 15: 292–303.
- Fujimoto N, Adachi-Usami E. Use of blue-on-yellow perimetry to demonstrate quadrantanopia in multiple sclerosis. *Arch Ophthalmol* 1998; 116: 828–9.
- Gabilondo I, Sepulveda M, Ortiz-Perez S, Fraga-Pumar E, Martinez-Lapiscina EH, Llufrui S, et al. Retrograde retinal damage after acute optic tract lesion in multiple sclerosis. *J Neurol Neurosurg Psychiatry* 2013; 84: 824–6.
- Green AJ, McQuaid S, Hauser SL, Allen IV, Lyness R. Ocular pathology in multiple sclerosis: retinal atrophy and inflammation irrespective of disease duration. *Brain* 2010; 133: 1591–601.
- Gündüz K, Cansu K, Buldukclar S, Saatçi I. Homonymous hemianopsia as the initial manifestation of multiple sclerosis. *Ophthalmologica* 1998; 212: 215–20.
- Khawaja AP, Chua S, Hysi PG, Georgoulas S, Curren H, Fitzgerald TW, et al. Comparison of associations with different macular inner retinal thickness parameters in a large cohort: the UK Biobank. *Ophthalmology* 2020; 127: 62–71.
- Kleerekooper I, Petzold A, Trip SA. Anterior visual system imaging to investigate energy failure in multiple sclerosis. *Brain* 2020; 143: 1999–2008.
- Ko F, Foster PJ, Strouthidis NG, Shweikh Y, Yang Q, Reisman CA, et al. Associations with retinal pigment epithelium thickness measures in a large cohort. *Ophthalmology* 2017; 124: 105–17.
- Lingsma HF, Roozenbeek B, Steyerberg EW, Murray GD, Maas AIR. Early prognosis in traumatic brain injury: from prophecies to predictions. *Lancet Neurol* 2010; 9: 543–54.
- London F, Zéphir H, Drumez E, Labreuche J, Hadhoum N, Lannoy J, et al. Optical coherence tomography: a window to the optic nerve in clinically isolated syndrome. *Brain* 2019; 142: 903–15.
- Lycke J, Tolleson PO, Frisén L. Asymptomatic visual loss in multiple sclerosis. *J Neurol* 2001; 248: 1079–86.
- Nielsen JM, Korteweg T, Barkhof F, Uitdehaag BMJ, Polman CH. Overdiagnosis of multiple sclerosis and magnetic resonance imaging criteria. *Ann Neurol* 2005; 58: 781–3.
- Nolan RC, Galetta SL, Frohman TC, Frohman EM, Calabresi PA, Castrillo-Viguera C, et al. Optimal intereye difference thresholds in retinal nerve fiber layer thickness for predicting a unilateral optic nerve lesion in multiple sclerosis. *J Neuro-Ophthalmol* 2018; 1.
- Nolan-Kenney RC, Liu M, Akhand O, Calabresi PA, Paul F, Petzold A, et al. Optimal intereye difference thresholds by optical coherence tomography in multiple sclerosis: an international study. *Ann Neurol* 2019; 85: 618–29.
- Oberwahrenbrock T, Traber GL, Lukas S, Gabilondo I, Nolan R, Songster C, et al. Multicenter reliability of semiautomatic retinal layer segmentation using OCT. *Neuro Immunol Neuroinflamm* 2018; 5: e449.
- Odom JV, Bach M, Brigell M, Holder GE, McCulloch DL, Mizota A, et al. ISCEV standard for clinical visual evoked potentials: (2016 update). *Doc Ophthalmol* 2016; 133: 1–9.
- Outteryck O, Lopes R, Drumez É, Labreuche J, Lannoy J, Hadhoum N, et al. Optical coherence tomography for detection of asymptomatic optic nerve lesions in clinically isolated syndrome. *Neurology* 2020; 95: e733–e744.
- Patel PJ, Foster PJ, Grossi CM, Keane PA, Ko F, Lotery A, et al. Spectral-domain optical coherence tomography imaging in 67 321 adults. *Ophthalmology* 2016; 123: 829–40.
- Petzold A. Intrathecal oligoclonal IgG synthesis in multiple sclerosis. *J Neuroimmunol* 2013; 262: 1–10.
- Petzold A, Balcer LJ, Calabresi PA, Costello F, Frohman TC, Frohman EM, et al. Retinal layer segmentation in multiple sclerosis: a systematic review and meta-analysis. *Lancet Neurol* 2017; 16: 797–812.
- Petzold A, de Boer JF, Schippling S, Vermersch P, Kardon R, Green A, et al. Optical coherence tomography in multiple sclerosis: a systematic review and meta-analysis. *Lancet Neurol* 2010; 9: 921–32.
- Petzold A, Wattjes MP, Costello F, Flores-Rivera J, Fraser CL, Fujihara K, et al. The investigation of acute optic neuritis: a review and proposed protocol. *Nat Rev Neurol* 2014; 10: 447–58.

- Pulicken M, Gordon-Lipkin E, Balcer LJ, Frohman E, Cutter G, Calabresi PA. Optical coherence tomography and disease subtype in multiple sclerosis. *Neurology* 2007; 69: 2085–92.
- Reich DS, Lucchinetti CF, Calabresi PA. Multiple sclerosis. *N Engl J Med* 2018; 378: 169–80.
- Riederer I, Mühlau M, Hoshi M-M, Zimmer C, Kleine JF. Detecting optic nerve lesions in clinically isolated syndrome and multiple sclerosis: double-inversion recovery magnetic resonance imaging in comparison with visually evoked potentials. *J Neurol* 2019; 266: 148–56.
- Saidha S, Syc SB, Ibrahim MA, Eckstein C, Warner CV, Farrell SK, et al. Primary retinal pathology in multiple sclerosis as detected by optical coherence tomography. *Brain* 2011; 134: 518–33.
- Seshan V, Gönen M, Begg C. Comparing ROC curves derived from regression models. *Stat Med* 2012; 32: 1483–93.
- Sinnecker T, Clarke MA, Meier D, Enzinger C, Calabrese M, Stefano ND, et al. Evaluation of the central vein sign as a diagnostic imaging biomarker in multiple sclerosis. *JAMA Neurol* 2019.
- Tewarie P, Balk L, Costello F, Green A, Martin R, Schippling S, et al. The OSCAR-IB consensus criteria for retinal OCT quality assessment. *PLoS ONE* 2012; 7: e34823.
- Thompson AJ, Banwell BL, Barkhof F, Carroll WM, Coetzee T, Comi G, et al. Diagnosis of multiple sclerosis: 2017 revisions of the McDonald criteria. *Lancet Neurol* 2018a; 162–73.
- Thompson AJ, Baranzini SE, Geurts J, Hemmer B, Ciccarelli O. Multiple sclerosis. *Lancet* 2018b; 391: 1622–36.
- Villoslada P, Sanchez-Dalmau B, Galetta S. Optical coherence tomography: a useful tool for identifying subclinical optic neuropathy in diagnosing multiple sclerosis. *Neurology* 2020; 95: 239–40.
- de Vries-Knoppert WA, Baaijen JC, Petzold A. Patterns of retrograde axonal degeneration in the visual system. *Brain* 2019; 142: 2775–86.
- Xu SC, Kardon RH, Leavitt JA, Flanagan EP, Pittock SJ, Chen JJ. Optical coherence tomography is highly sensitive in detecting prior optic neuritis. *Neurology* 2019; 92: e527–e535.